SAFETY WINDOWS: KNOWLEDGE MAPS FOR ACCIDENT PREDICTION AND PREVENTION IN MULTIFACTOR FLIGHT SITUATIONS

I.Y. Burdun
INTELONICS Ltd.

Keywords: *multifactor flight situations, safety protection*

Abstract

Safety windows are intelligent formats specially designed to depict system-level knowledge of aircraft flight physics and logic in complex (multifactor) situations. This knowledge is extracted from fast-time 'what-if' modeling and simulation (M&S) experiments. VATES tool (Virtual Autonomous Test and Evaluation Simulator, v.7) is employed as 'knowledge generator'. The safety window concept is used to support a 'bird's eye view' level mapping, analysis, prediction and protection of an aircraft's flight safety under uncertainty. The goal is to indentify, study, and avoid potentially dangerous anomalies in the 'operator (pilot, automaton) – aircraft – operational environment' system behavior in advance, before the situation may become irreversible.

1 Introduction

1.1 The Problem

A complex (multifactor) situation can quickly develop in apparently normal flight as a result of unfavorable mixing and dynamic cross-coupling of several demanding operational circumstances and design shortcomings linked by strong (physics- and logic-based) cause-and-effect relationships. These multifactor combinations typically lead to a 'chain-reaction' type accident or incident (Fig. 1).

The following operational and design factors can contribute to spontaneous development of a complex situation in flight:

- a human pilot's errors, pilot inattention or deliberately unsafe actions; variations in piloting techniques and tactics
- mechanical malfunctions and automatic control software logic flaws and data errors in onboard systems
- demanding weather and terrain conditions (wind-shear, microburst, heavy rain, cross-wind, wet runway, atmospheric turbulence, in-flight icing, natural and urban obstacles, etc.), and
- substantial variations in flight mission setup parameters (aerodynamic configuration, center of gravity (C.G.) position, flying mode, etc.).

In spite of a negligibly small probability of occurrence, multifactor accidents do happen in flight operation. Their logical and physical patterns are very unusual (even anomalous), poorly documented and under-tested.

There exists a sub-domain of theoretically implausible but practically viable multifactor flight accident scenarios. At present, these scenarios cannot be blocked or remedied reliably in operation. Multifactor cases are difficult to examine exhaustively during design, test and certification/evaluation due to combinatorial, technical, time and budget constraints. A generalized yet affordable technique is therefore needed for flight safety prediction and protection in complex (multifactor) flight situations.

1.2 The Solution Approach

'Knowledge is Power'. Basically, the root cause of a human operator's (or automaton's) failure in a multifactor situation is probably hidden in

the information gaps and structural flaws of his/her (its) internal 'knowledge base'. Ideally, this knowledge system should account for non-linear, multi-variant character of aircraft dynamics (input-sensitive, branching flight paths) under complex conditions. It should also include information on both safe and unsafe control tactics in such situations.

A new methodology has been developed to help study and enhance aircraft safety performance under multifactor conditions by exploring and mapping, in advance, key physical and logical relationships of flight.

1.3 Research Task Formulation

The research task can be formulated as follows:

- develop a technique capable of deriving a priori systemic knowledge that represents key relationships of flight on a 'bird's eye view' level for a broad range of potentially unsafe multifactor flight scenarios
- design a set of anthropomorphic formats to help memorize this knowledge in a specialist's long-term memory, and
- carry out a proof-of-concept case study to demonstrate the feasibility of a 'knowledge-centered' technology for flight safety prediction and protection

2 Theoretical Framework of Multifactor Flight Domain Knowledge Model

2.1 Key Concepts for Complex Flight Domain M&S

A generalized conceptual M&S framework has been developed for aircraft safety performance mapping, analysis, prediction and protection under multifactor conditions. These concepts are independent of aircraft type, flight situation and operational conditions.

The developed framework includes the following key concepts [1-4]: system model, event, process, scenario, micro- and macro-structure of flight, baseline scenario, operational (design) factor, operational hypothesis, situational tree, safety palette, partial safety spectra, integral safety spectrum, safety

classification categories, safety chances distribution pie chart, safety window, safety 'topology', family of integral safety spectra of a situational tree, dynamic safety window, safety chances distribution time-history, etc.

2.2 Flight M&S Output Measurement

The 'operator (pilot, automaton) – aircraft – operational environment' system (the system) behavior is described as a chronologically ordered set of system states $x(t)$,

$$x(t) = \{x_1(t), \ldots, x_i(t), \ldots, x_{N(x)}(t)\}, \qquad (1)$$

where x_i is a system variable, $x_i \in x$, $t \in [t_*; t^*]$.

This sequence is called a 'flight' F_k,

$$F_k = \{\{x_1(t_*), \ldots, x_{N(x)}(t_*)\}, \ldots, \{x_1(t_* + \qquad (2)$$
$$(n-1) \cdot \Delta), \ldots, x_{N(x)}(t_* + (n-1) \cdot \Delta)\}\},$$

where n is the total number of records in F_k, $t^* = t_* + (n-1) \cdot \Delta$, and Δ is the time increment of M&S data recording in the set (file) F.

2.3 Micro- and Macro-Structure of Flight

Safety related knowledge of a multifactor flight situation domain is studied on two interconnected levels. These are the 'micro-structure' of flight (a flight situation scenario) and the 'macro-structure' of flight (a situational tree of flight). The relationship between these two knowledge structures is shown in Fig. 2.

The micro-structure of flight is a generalized model of a stand-alone (single) flight situation. It is represented by the concept of fight situation scenario. The latter is basically an oriented (directed) graph, which consists of interconnected events and processes. In the scenario graph, events (vertices) stand for discrete components of a flight situation model, whilst processes (oriented arcs) stand for its continuous components. The formal scenario is preplanned, and it must capture key cause-and-effect and other logic relationships of flight dynamics and control.

The macro-structure of flight is a generalized knowledge model of a family of neighboring ('what-if') situations. It is represented, planted, stored and used in safety analysis as a situational tree. The tree trunk

stands for a given baseline flight situation scenario – standard or non-standard one. Secondary n^{th}-order (derivative) branches represent multifactor situation scenarios, which implement meaningful variations of the baseline scenario or derivative scenarios of a lower level. New branches are automatically 'implanted' into a tree using VATES (v.7) tool [5].

2.4 Baseline Situation Scenarios (Examples)

Examples of various takeoff situation scenarios are shown in Table 1. Each of these takeoff cases is used as a baseline situation scenario to plant a special situational tree in M&S experiment.

Table 1. Baseline Situation Scenarios

S_1	Normal takeoff, benign weather (ground-roll, lift-off, and initial climb
S_2	Normal takeoff, cross-wind conditions and slippery runway (ground-roll, lift-off, and initial climb)
S_3	Continued takeoff, one engine out at V_{EF} (ground-roll, lift-off, and initial climb)
S_4	Normal takeoff, wind-shear conditions, (ground-roll, lift-off, and initial climb)
S_5	Continued takeoff, cross-wind conditions, engine out at V_{EF} (ground-roll, lift-off, and initial climb)
S_6	Low-altitude flight (climb, level flight or descent in the vicinity of urban infra-structure obstacles)

A joint graph of the six baseline situation scenarios listed above is shown in Fig. 5. It follows from the figure that the concept of scenario graph is a universal structure suitable for clear and concise representation of flight situations of any complexity level. Though the scenarios S_1, …, S_6 are structurally close they represent different flight situations. Scenario graphs can be easily modified – by adding new events and processes or by changing the parameters of existing components.

2.5 Operational Factor

The operational (or design) factor Φ is some event or process (or its attribute), which can be added to or withdrawn from a baseline (or derivative) flight situation scenario. Operational factors can vary substantially, independently or cross-coupled, and thus improve or deteriorate the aircraft safety performance.

Typically, an operational factor Φ is defined by a single system variable x_i, $x_i \in x$.

Operational factors are used in M&S experiments to create multifactor derivative ('neighboring') branches in a situational tree – specially designed variations of a baseline situation. Each derivative 'flight' from the tree corresponds to one combination of operational factors Φ_j.

2.6 Operational Hypothesis

An operational factor alone is not critically dangerous. It is much more important to study in advance the effects of various combinations of operational factors on flight safety. A meaningful combination of several operational factors is called the operational hypothesis.

The operational hypothesis Γ is a formal rule used to incorporate a new complex of operational factors into a baseline scenario. In short, the operational hypothesis can be defined as follows:

$$\Gamma = \prod_{i=1}^{n}\left[\sum_{k=1}^{m}\Phi_k^i\right] \qquad (3)$$

where Φ^i_k is the kth dependent factor added to the baseline scenario on the ith independent level of the situational tree branching process, $i = 1, …, n$, $k = 1, …m$. Π is the symbol of Cartesian product, and Σ is the symbol of dependent (cross-coupled) combination of operational factor values Φ_k^i on the ith level.

A design field of the operational hypotheses $\{\Gamma_1, …, \Gamma_{14}\}$ to be linked to the baseline flight situation scenarios S_1, …, S_6 (including takeoff, initial climb, low-altitude level flight, or descent modes) is depicted in Fig. 6. This diagram also contains the operational factors $\{\Phi_1, …, \Phi_{13}\}$ selected for virtual testing in M&S experiments.

2.7 Situational Tree as Knowledge Base of Multifactor Flight Domain

A composition of a baseline scenario S and an operational hypothesis Γ in a M&S experiment, $S \cdot \Gamma$, results in a structured set of 'neighboring' situations ('flights'), or a situational ('what-if') tree T:

$$T = S \cdot \Gamma \equiv \Omega(F). \qquad (4)$$

In other words, the rule (3) can be viewed as the tree (4) 'genotype', which determines its shape, size, and branching properties. Each situation-branch B_k (a 'flight' F_{ik}), $B_k \in T$, is defined by a subset of contributing factors Φ_j (the rule Γ), baseline scenario S and the system dynamics.

The overall goal of constructing situational trees is to examine combined effects of various operational (and possibly design) factors on an aircraft's safety performance and thus generate missing virtual statistics on multifactor accident patterns in advance.

The sources of information to quantify operational factors for M&S are national airworthiness requirements, FMEA reports, flight test and certification programs, flight operation statistics, accident/incident reports.

The goal of M&S based virtual flight test and certification (evaluation) is to construct a 'forest' of situational trees and analyze safety properties of the complex flight situation domain it threads based on design, test, operation, and incident/accident data.

2.8 Human Pilot's Situational Experience and Fractal Analogy

It can be argued that a human pilot's situational (tactical) experience is stored in his/her long-term memory in the logical form of a 'situational tree'. Like a fruit tree, a human pilot's internal 'situational tree' requires special care. This process should include the following main tasks: shape and trim the tree 'crown', 'graft' new branches, reconstruct lost or missing components, cut useless shoots. The goal is to obtain, for a given aircraft type and flight mission, a competent, efficient yet economic and quickly accessible system of knowledge that corresponds to the domain of anticipated complex (multifactor) flight conditions.

The growth dynamics of a fractal tree (Fig. 3) is a good illustration of a multi-stage process of the situational experience development and refinement in a pilot's long-term memory. Fig. 4 depicts a natural fractal tree, which can be considered as a model of the main structural and logical defects of a human pilot's situational knowledge system: missing knowledge, forgotten or shadowed knowledge, chaotic knowledge, and fragmentary knowledge.

Ideally, future technologies for flight safety protection must be capable to back up these weaknesses of a human pilot. At the same time, new techniques must take into account well-known strengths of a human pilot's decision-making mechanism. One of the goals is to strengthen a human pilot's real-time predictive capability in multifactor situations by employing unique properties of M&S and AI.

2.9 Safety Palette. Fuzzy Flight Constraints

Color is natural and, perhaps, the most effective and efficient medium for storing and communicating safety-related information to/ from an operator (a pilot or automaton). Five basic colors (green, yellow, red, black and grey) are used to denote respectively 'normal', 'warning', 'dangerous', 'catastrophic' and 'uncertain' levels of the system safety state for each measured system variable x_i from (1) and each time instant t recorded in flight – see Fig. 7(a).

Operational constraints of flight under multifactor conditions are not known precisely. They are inherently fuzzy. The notion of fuzzy constraint first introduced by Prof. L.A. Zadeh is employed for approximate measurement of the compatibility of current system states (i.e. measured at time instants t) with operational constraints using key system variables (monitored flight parameters).

A notional example of the fuzzy constraint for the angle of attack (AoA) variable is presented in Fig. 7(b), together with a scheme for coloring its numeric definition domain using the flight safety palette.

2.10 Safety Spectra

For each flight situation from a situational tree, current safety levels can be measured for all monitored variables x_k at all recorded time instants as shown in Fig. 8 using 'flight' F_{2782}: "Normal takeoff, initial climb at $\theta_g=16^o$ and $\gamma_g=22.5^o$, 'very strong' wind-shear" as an example.

The integral safety spectrum is a color-coded situation safety time-history, in which all cases of the violation of fuzzy constrains are found and mapped at the 'hottest' level taking into account the available partial safety spectra.

As a result, for each situation from the tree, a family of partial safety spectra Σ_k, $k = 1, \ldots, p,$ and an integral safety spectrum Σ can be constructed. More details on the algorithm of flight safety spectra construction and its applications can be found in [1-4].

An example of the situational tree $S_1 \cdot \Gamma_{11}$: "Takeoff and initial climb, 'strong' wind-shear, flight path and bank angles control errors" is depicted in Fig. 9. The tree's branches (flight paths) are colored in the integral safety spectra.

2.11 Safety Classification Categories

One more level of flight safety knowledge generalization is needed. The goal is to measure the aircraft's safety performance in a particular flight situation as a whole.

With this purpose, a generalized 'safety ruler' that consists of six safety classification categories is introduced (Table 2).

Table 2. Safety Classification Categories

Code	Name	Safety Category Definition Criterion
I	Safe	The system state resides mainly inside the 'green' zone. As a maximum, the system state may stay, for a short time in close proximity to the operational constraints, i.e. inside the 'yellow' zone, but must leave it by the end of the situation
II-a	Conditionally Safe – a	As a maximum, the system state may stay temporarily, or for a medium time, in close proximity to the operational constraints, i.e. inside the 'yellow' zone
II-b	Conditionally Safe – b	As a maximum, the system state may stay for a long time in close proximity to the operational constraints, i.e. inside the 'yellow' zone
III	Potentially Unsafe	As a maximum, the system state may violate operational constraints, i.e. enter the 'red' zone, for a short or between short and medium time, but must leave it by the end of the situation
IV	Dangerous (Prohibited)	As a maximum, the system state may stay beyond the operational constraints, i.e. inside the 'red' zone, for a medium or long time or till the end of the situation
V	Catastrophic ('Chain Reaction')	There is at least one (i.e. for a very short time) occurrence of the violation of any operational constraint at the 'black' level

This safety classification principle takes into account the palette, 'weight' and position of the four basic safety colors $\{\xi_G, \xi_Y, \xi_R, \xi_B\}$ in the integral safety spectrum Σ of a flight situation F_{ik} to be evaluated, $F_{ik} \in \Omega(F)$.

Two new colors ('salad green' and 'orange') have been added to the original safety palette in order to denote interim categories **II-a** and **III**, respectively.

The selected total number of the flight safety classification categories in Table 2 (six) in general corresponds to a human expert's ability to reliably recognize and utilize not more than 5-10 gradations of a complex, difficult-to-formalize system-level property. Additional, or more refined, categories with interim colour coding can be added if necessary. This approach is based on the concept of 'information granulation' introduced by Prof. L.A. Zadeh.

The main criterion of assigning a safety category to a specific situation is the relative duration of the aircraft state residence, respectively, in the 'green', 'salad green', …, 'black' zone of this situation's integral safety spectrum.

As a result, for each situation from the tree, a qualitative safety level (flight safety category) can be assigned. This generalized color code ('safety grade') will be used for flight safety analysis and decision-making in complex situations.

2.12 Safety Chances Distribution Chart

A distribution of safety chances $\{\chi^I, \chi^{II-a}, \chi^{II-b}, \chi^{III}, \chi^{IV}, \chi^V\}$ can be calculated for the six clusters of derivative situations which constitute a situational tree T. It indicates how many situations of each safety category are present in a particular tree. In other words, the safety chances distribution chart is a map of the aircraft's inherent safety performance for a combination of a given operational hypothesis (Γ) and a given baseline scenario (S).

2.13 Safety Window

Let us have a tree of 'flights' $\Omega(F)$, $\Omega(F) = \{F_{(1),(1)}, \ldots, F_{(i),(j)}, \ldots, F_{(m),(n)}\}$ with the following pairs of values for two key operational factors Φ_a and Φ_b: $\{(\Phi_{a(1)}, \Phi_{b(1)}), \ldots, (\Phi_{a(i)}, \Phi_{b(j)}), \ldots, (\Phi_{a(m)}, \Phi_{b(n)})\}$, where $\Phi_{a(1)} > \Phi_{a(2)} > \ldots > \Phi_{a(m)}$ is a top-to-bottom vertical ordering relation for values of the first factor Φ_a and $\Phi_{b(1)} < \Phi_{b(2)} < \ldots < \Phi_{b(n)}$ is a left-to-right horizontal ordering relation for values of the second key factor Φ_b.

Then the flight safety window can be defined as a $m \times n$ matrix $W(\Phi_a, \Phi_b)$ with coordinates Φ_a and Φ_b, where w_{ij} is a cell located on the crossing of the row #i and column #j, $w_{ij} = [(\Phi_{a(i)}, \Phi_{b(j)}), \xi^k_{ij}]$, $i = 1, \ldots, m, j = 1, \ldots, n, k \in \{I, \ldots, V\}$. The cell w_{ij} contains the following information:

- $\Phi_{a(i)}, \Phi_{b(j)})$ – a pair of values of factors (Φ_a, Φ_b), where $\Phi_{a(i)} = const$ for $(\forall i)$ ($i = 1, \ldots, m$) and $\Phi_{b(j)} = const$ for $(\forall j)$ ($j = 1, \ldots, n$), and
- ξ^k_{ij} – the color of the kth cluster, which the 'flight' $F_{(i),(j)}$ belongs to, $k \in \{I, \ldots, V\}$, $\xi^k_{ij} \in \{\xi^I, \ldots, \xi^V\}$.

The VATES tool incorporates an algorithm for automatic mapping of all 'flights' from a tree $\Omega(F)$, $\Omega(F) = S \cdot \Gamma$, on to a safety window plane $W(\Phi_a, \Phi_b)$.

2.14 Flight Safety 'Topology'

Analyses of a large number of various safety window patterns have resulted in the concept of flight safety topology.

Given a situational tree $\Omega(F)$, $\Omega(F) = S \cdot \Gamma$, and its safety window $W(\Phi_a, \Phi_b)$, the aircraft's safety performance can be graded according to the categories $\{I, \ldots, V\}$, where $\Phi_a, \Phi_b \in \{\Phi_{j(1)}, \ldots, \Phi_{j(N(\Phi))}\}$. Then, in the window $W(\Phi_a, \Phi_b)$ the following characteristic topological objects can be identified (Fig. 10): the 'abyss' **1** (a catastrophe); the 'hill' **2** (a danger); the 'slope' **3** (a reversible state transition); the 'valley' **4** (standard safety situations); the 'lake' **5** (maximum safety, or optimum situations); and the 'precipice' **6** (abrupt, irreversible state transitions, 'chain reaction').

An integrated color graphic image of the mutual arrangement and inter-dependence of the above-listed objects in the safety window $W(\Phi_a, \Phi_b)$ is called the safety 'topology' of a multifactor flight situation domain with two key operational factors (Φ_a, Φ_b) selected for monitoring.

The 'abyss' is a subset of neighboring – in projection on the window $W(\Phi_a, \Phi_b)$ plane – 'flights', which represent catastrophic scenarios. These situations are treated as Category **V** cases and painted in black color ξ^V. The 'hill' is a subset of neighboring – in projection on the window $W(\Phi_a, \Phi_b)$ plane – 'flights', which are known as dangerous scenarios. These situations are rated as Category **IV** cases and painted in red color ξ^{IV}.

The 'slope' or 'foot' is a subset of transitional situations, which link together a 'valley' and a 'hill' – smoothly and by a shortest way – in projection on the window $W(\Phi_a, \Phi_b)$ plane. They are rated as Category **II-b** and **III** cases: $((\xi^I \lor \xi^{II-a}) \to (\xi^{II-b} \lor \xi^{III}) \to (\xi^{IV})) \Rightarrow$ 'slope'. Normally, the 'slope'-type situations are reversible; they must be known and routinely managed in flight operations.

The 'valley' is a subset of neighboring – in projection on the window $W(\Phi_a, \Phi_b)$ plane – 'flights' which represent standard, normal safety scenarios. They are rated as Category **I** and **II-a** cases and painted in green and light-green colors (ξ^I, ξ^{II-a}), respectively. The 'lake' is a subset of neighboring – in projection on the window $W(\Phi_a, \Phi_b)$ plane – 'flights', which are considered as optimal scenarios maximizing the vehicle's safety performance or mission effectiveness. Normally, they belong to Category **I** and Category **II-a** and are painted in turquoise color ξ_T. Finally, the 'precipice' is a subset of abrupt transitions from a 'valley'/'hill' to an 'abyss'. They are assessed as Category **V** cases and represent catastrophic developments of flight: $(((\xi^I \lor \xi^{II-a}) \to \xi^V) \lor (\xi^{IV} \to \xi^V)) \Rightarrow$ 'precipice'. The precipice type transitions are irreversible, i.e. prone to a 'chain reaction' accident. Therefore, they must be reliably prevented (avoided) in flight operations and their precursors must be tested in advance.

2.15 Dynamic (Time-Dependent) Safety Window

Let us assume that an aircraft is equipped with a multi-modal sensor suit capable of real-time measurements of the two key factors (Φ_a, Φ_b) and a third, possibly time-critical, key factor Φ_c.

Then a sequence of safety windows, $W(\Phi_a,\Phi_b)|t_0$, $W(\Phi_a,\Phi_b)|t_1$, $W(\Phi_a,\Phi_b)|t_2$, ..., can be constructed for a series of consecutive time instants $\{t_0, t_1, t_2, ...\}$. This sequence, $W(\Phi_a,\Phi_b)|t_i \wedge \Phi_c = \Phi_c(t_i)$, $t_i = t_0, t_1, t_2, ...$, is called the dynamic (time-dependent) safety window, $W(\Phi_a, \Phi_b, \Phi_c) = f(t)$. It can be used to map additional impact of the third, time-critical, factor Φ_c on the aircraft's safety performance under the operational hypothesis $\Phi_a \times \Phi_b$.

A virtual environment that ergonomically implements the sequence $W(\Phi_a, \Phi_b, \Phi_c) = f(t)$ in fact represents a prototype of an intelligent pilot-vehicle interface system for active safety management under multifactor conditions [1-4].

2.16 'Last Chance for Recovery' Point

Given a flight safety prediction time range $[t_0; t_0 + \Delta_P]$, $[t_0; t_0 + \Delta_P] \subset [t_*; t^*]$, and a triple of key factors $\{\Phi_a, \Phi_b, \Phi_c\}$, $\{\Phi_a, \Phi_b, \Phi_c\} \subset \Omega(\Phi)$, a sub-tree T' that emerges from the current situation can be dynamically extracted from T and processed onboard (Fig. 9), where t_0 is the safety prediction start point measured with respect to the current flight time t and Δ_P is the depth of safety predictions, $\Delta_P \in [3; 30]$ s.

Then for the situations from T' it becomes possible to calculate the probability $(\chi^{\mathbf{IV}} + \chi^{\mathbf{V}})$ of the event that the system state will enter the zones $\xi^{\mathbf{IV}}$ and $\xi^{\mathbf{V}}$ during the prediction time range $[t_0; t_0 + \Delta_P]$. If $(\chi^{\mathbf{IV}} + \chi^{\mathbf{V}}) > \chi_{max}$ this means that a catastrophic development of the current situation is imminent, where χ_{max} is the threshold for safety protection decision-making.

The value of χ_{max} determines the 'last chance for recovery' point $t_\uparrow$. At this point, it is mandatory for the operator to abort current automatic control or piloting tactics and immediately implement a new control scenario for restoring flight safety. It is essential that short-term safety forecasts and recovery control selection decisions are based on the systematic knowledge of flight physics and logic stored in the situational tree T.

2.17 Safety Restoring Scenario

Given an emergency in flight, a safety restoring (recovery control) scenario $S_\uparrow$ must be applied to the aircraft beginning from the 'last chance for recovery' point $t_\uparrow$. This is a scenario of the safest possible branch from T' that continues the current situation and moves the vehicle away from 'abyss' type transitions in the safety window.

The recovery scenario $S_\uparrow$ can be implemented either automatically or manually. This depends on the complexity level of a current situation, mission type, aircraft class and technical condition, phase of flight, operator qualification (competence) and physical (technical) condition, etc. In the manual recovery mode, key parameters of the safety restoring scenario $S_\uparrow$ can be entered by means of a tactile display containing a dynamic window $W(\Phi_a, \Phi_b, \Phi_c(t))$ or using other advanced pilot-vehicle interface technologies[1]. In the automatic recovery mode, these parameters are derived from the onboard knowledge base – a 'forest' of situational trees, $\Omega(T)$.

2.18 Active Safety Management

A generic algorithm for active management of flight safety under multifactor conditions has been developed using the formal framework introduced above. The algorithm input data set includes the following [3]: $\{\Omega(T), \Omega(\Phi), \Omega(\Gamma), \Omega^M(\Phi), \{\Phi_a, \Phi_b, \Phi_c\}, \Omega(C), x', t_0, \Delta_P, T', \chi^{\mathbf{IV}}, \chi^{\mathbf{V}}, ...\}$, where $\Omega^M(\Phi)$ is the subset of key operational factors selected for real-time monitoring and aircraft's safety performance prediction during a given phase of flight, $\Omega^M(\Phi) = f(t)$, $\{\Phi_a, \Phi_b, \Phi_c\} \subset \Omega(\Phi)$, $\Phi_a, \Phi_b, \Phi_c = f(t)$, $\Omega(C)$ is the set of monitored fuzzy constraints, $T' \subset T$, and x' is the subset of key monitored system variables, $x' \subset x$.

By tuning these parameters (primarily – $\Omega(\Gamma)$, $\Omega^M(\Phi)$, $\{\Phi_a, \Phi_b, \Phi_c\}$, t_0 and Δ_P), a

flexible, adaptive policy of proactive flight safety management can be tailored to account for the strengths and weaknesses in the 'knowledge base' of a specific human pilot or automaton type.

3 Simulation Results Discussion

3.1 Experiment Setup

A series of M&S experiments has been carried out with the system model for takeoff, climb, level and descent flight modes of a notional commuter airplane using the methodology described above.

Some 1500 multifactor situations have been examined in M&S. Six baseline scenarios $\{S_1, ..., S_6\}$ have been constructed and simulated (Fig. 6). A large set (13) of operational factors have been formalized for testing (Fig. 7), $\Omega(\Phi) = \{\Phi_1, ..., \Phi_{13}\}$. In total, 14 realistic multifactor operational hypotheses have been designed and tested in M&S (Fig. 7), $\Omega(\Gamma) = \{\Gamma_1, ..., \Gamma_{14}\}$, where: $\Gamma_1 = \Phi_1 \times (\Phi_2 + \Phi_3) \equiv \overline{x}_{CG} \times (V_R + \Delta\delta_e)$, $\Gamma_2 = \Phi_5 \times \Phi_4 \equiv W_{yg} \times \mu$, $\Gamma_3 = \Phi_1 \times (\Phi_7 + \Phi_8) \times \Phi_6 \equiv \overline{x}_{CG} \times (\theta_{G1} + \theta_{G2}) \times H_{FL}$ ($\overline{x}_{CG} = \overline{x}_{CG\min}$), $\Gamma_4 = \Phi_1 \times (\Phi_7 + \Phi_8) \times \Phi_6 \equiv \overline{x}_{CG} \times (\theta_{G1} + \theta_{G2}) \times H_{FL}$ ($\overline{x}_{CG} = \overline{x}_{CG\max}$), $\Gamma_5 = \Phi_{13} \times \Phi_7 \times \Phi_8 \equiv \zeta_{LHE} \times \theta_{G1} \times \theta_{G2}$ ($V_{EF} = 150$ km/h), $\Gamma_6 = \Phi_9 \times \Phi_6 \equiv k_W \times H_{FL}$, $\Gamma_7 = \Phi_1 \times \Phi_9 \times (\Phi_7 + \Phi_8) \equiv \overline{x}_{CG} \times k_W \times (\theta_{G1} + \theta_{G2})$ ($\overline{x}_{CG} = \overline{x}_{CG\min}$), $\Gamma_8 = \Phi_{10} \times \Phi_7 \times \Phi_8 \equiv k_P \times \theta_{G1} \times \theta_{G2}$, $\Gamma_9 = \Phi_2 \times \Phi_{10} \times \Phi_7 \times \Phi_{11} \equiv V_R \times k_P \times \theta_{G1} \times \gamma_G$, $\Gamma_{10} = \Phi_{13} \times \Phi_{12} \times \Phi_4 \equiv \zeta_{LHE} \times V_{EF} \times W_{yg}$, $\Gamma_{11} = \Phi_7 \times \Phi_{11} \equiv \theta_{G1} \times \gamma_G$, $\Gamma_{12} = \Phi_9 \times \Phi_7 \times \Phi_{11} \equiv k_W \times \theta_{G1} \times \gamma_G$ ($k_W = 1$), $\Gamma_{13} = \Phi_9 \times \Phi_7 \times \Phi_{11} \equiv k_W \times \theta_{G1} \times \gamma_G$ ($k_W = 1.5$).

In order to monitor and assess the aircraft's safety performance 20 fuzzy constraints have been defined for a subset x' of key system variables x_k, $x' = \{V_{IAS}, \beta, n_z, E, N, \gamma, \vartheta, V_{zg}, \alpha, k_{LG}, \delta_e, \delta_a, \delta_r, \delta_F, ...\}$.

Finally, the following compositions of baseline takeoff, level flight and descent scenarios S_i, $S_i \in \Omega(S)$, and operational hypotheses Γ_k, $\Gamma_k \in \Omega(\Gamma)$, have been examined in M&S: $S_1 \cdot \Gamma_1$, $S_2 \cdot \Gamma_2$, $S_1 \cdot \Gamma_3$, $S_1 \cdot \Gamma_4$, $S_3 \cdot \Gamma_5$, $S_4 \cdot \Gamma_6$, $S_4 \cdot \Gamma_7$, $S_1 \cdot \Gamma_8$, $S_1 \cdot \Gamma_9$, $S_5 \cdot \Gamma_{10}$, $S_1 \cdot \Gamma_{11}$, $S_4 \cdot \Gamma_{12}$, $S_4 \cdot \Gamma_{13}$, and $S_6 \cdot \Gamma_{14}$. Selected results of these M&S experiments are presented and discussed below.

A special case study on the systemic safety analysis of a hypothetical low-altitude flight in the presence of a tower-type urban obstacle of unknown location is described in [1, 3]. This study relates to the composition $S_6 \cdot \Gamma_{14}$, which maps a sub-domain of climb, level flight and descent modes of a notional airliner flying in clean configuration at $V_{IAS} \in [320; 360]$ km/h and $H \in [200; 400]$ m. The resulting situational tree $S_6 \cdot \Gamma_{14}$ represents a set hypothetical situations with various combinations of the commanded flight path and bank angles: $\theta_{G2} \in \{-12°, ..., +24°\}$ and $\gamma_G \in \{-45°, ..., +45°\}$. Two alternative scenarios are analyzed [1, 3]: $S_0 \cup S_\downarrow$ and $S_0 \cup S_\uparrow$. They correspond, respectively, to a terrorist- (or fool-) type control and safety protection AI control based on a self-preservation imperative.

3.2 Takeoff Safety 'Topology' Mapping and Analysis

In Fig. 11, flight safety windows and safety chances distribution charts are depicted for the following multifactor compositions: $S_2 \cdot \Gamma_2$, $S_3 \cdot \Gamma_5$, $S_4 \cdot \Gamma_6$, $S_4 \cdot \Gamma_7$, $S_1 \cdot \Gamma_8$, $S_1 \cdot \Gamma_9$, $S_5 \cdot \Gamma_{10}$, $S_4 \cdot \Gamma_{12}$, and $S_4 \cdot \Gamma_{13}$.

In particular, in the composition $S_2 \cdot \Gamma_2$ the safety window W (Φ_4, Φ_5) contains one central green 'valley', two side red 'hills' and two connecting 'slopes' , where $\Phi_4 \equiv \mu$ and $\Phi_5 \equiv W_{yg}$. A steep 'slope' is observed in a ground-roll motion mode for dry and semi-wet runway surface conditions. A more gradual transition between safe and unsafe situations can be noticed for wet and water-covered runways. The shape and position of a 'cross-wind velocity – adhesion factor' operational constraint are visually identifiable. Scenario variants with strong cross-wind velocities of |15|…|20| m/s can be dangerous during ground-roll. These cases constitute 45% of all the cases constituting $S_2 \cdot \Gamma_2$. The remaining situations are safe and belong to Categories I and II.

In the composition $S_4 \cdot \Gamma_6$, the safety window W (Φ_9, Φ_6) maps a sub-domain of

takeoff situations under severe unsteady wind conditions. The commanded flight path angles in S_4 are $\theta_{G1}/\theta_{G2} = 8^o/8^o$. If a 'strong' or worse wind-shear is expected ($k_W \geq 1$) takeoff must be prohibited. In order to evaluate a possibility of safer outcomes at moderate wind-shear effects ($k_W < 1$), it is expedient to expand the flight safety window downward. If the aircraft unintentionally enters a zone of 'very strong' wind-shear with $k_W = 1.2 \ldots 1.6$, flaps must be retracted as late as possible to stay within the right-hand 'orange' zone. In overall, the chances of a catastrophe in the multifactor domain $S_4 \cdot \Gamma_6$ are high: ($\chi^{IV} + \chi^V) \approx 70\%$.

In the composition $S_4 \cdot \Gamma_7$, the safety 'topology' map includes a small green 'valley' at a lower left-hand corner of the window, a wide ($\Delta\Phi_9$ (ξ^{III}) ≈ 0.6) orange 'slope' above it followed by an extensive red 'hill' ($\chi^{IV} = 37\%$) adjacent to a black 'abyss' at the upper right-hand corner. The most dangerous transition can occur at $\theta_{G1}/\theta_{G2} = 6^o/8^o$ if the wind-shear intensity increases from ($k_W > 1.6$). These observations can be helpful to dynamically define robust piloting goals and constraints for (θ_{G1}, θ_{G2}) as a function of the wind-shear intensity. In particular, at takeoff under 'strong' and 'very strong' wind-shear ($1 < k_W \leq 1.6$), the maximum available safety level is achieved at $\theta_{G1}/\theta_{G2} = 5^o/3^o$. It is prohibited to climb at $\theta_{G1}/\theta_{G2} > 7^o/5^o$, and irreversible transitions are likely at $\theta_{G1} \geq 12^o$.

In the composition $S_5 \cdot \Gamma_{10}$, the safety window W (Φ_{12}, Φ_5) incorporates a wide central 'valley' and two side 'hills'. A large enough 'abyss' occupies the lower left-hand corner adjacent to the left-hand 'hill' and the central 'valley'. It is emerged at small and medium values of V_{EF}, $V_{EF} \in [100; 145]$ km/h, and is linked to the 'valley' by a 'precipice' type transitions 6. A small 'abyss' is also revealed at cross-wind of about 18 m/s for $V_{EF} \in [175; 190]$ km/h.

It follows from the composition $S_4 \cdot \Gamma_{12}$ (the window W (Φ_7, Φ_{11})) that a 'strong' wind-shear in climb can sharply degrade the aircraft's safety at small commanded flight path angles ($\theta_{G1} \leq 4^o$). The safety 'topology' picture calculated for 'strong' wind-shear effects

contains a stable catastrophic 'abyss' (a black strip in the bottom of W (Φ_7, Φ_{11})) and 'precipice' transitions 6 for small θ_{G1} and any commanded bank angle γ_G. It means that an attempt to perform initial climb at small flight path angles ($2^o \ldots 4^o$) inevitably leads to a fatal outcome.

Flight safety 'topology' obtained for 'very strong' wind-shear conditions ($S_4 \cdot \Gamma_{13}$) at small θ_{G1} and any γ_G contains a stable catastrophic 'abyss' (black strip in the bottom) and ''precipice' type transitions (6). That is, an attempt of initial climb at small flight path angles ($2^o \ldots 4^o$) would inevitably lead the vehicle to a fatal state.

In the composition $S_3 \cdot \Gamma_5$, if the left-hand engine fails during ground-roll (at $V_{EF} = 150$ km/h), then takeoff safety cannot be secured at commanded flight path angles $\theta_{G1} \geq 5^o$ (during initial climb). For the examined sub-domain of operational factors, the share of safe situations is equal to 36% but the share of potentially catastrophic situations is 43%. Failure of the left-hand engine during ground-roll decreases the upper limit of flight path angle in initial climb from $\theta_{G1} = 10^o \ldots 12^o$ in the composition $S_1 \cdot \Gamma_3$ (not shown here) to $2^o \ldots 4^o$. A 'precipice' type transitions (6) are observed at $\theta_{G2} = 0^o$. The 'abyss' type states are likely to occur at flight path angles $\theta_{G1} > 4^o$ (initial climb) for any θ_{G2} (2nd phase of climb).

The compositions Γ_8 and Γ_9 are used to check three- and four-factor sub-domains of flight, respectively (see Fig. 11), where $\Gamma_8 = k_P \times \theta_{G1} \times \theta_{G2}$ and $\Gamma_9 = V_R \times k_P \times \theta_{G1} \times \gamma_G$. The integrated effect of reduced thrust at takeoff, increased flight path angles in initial climb, and variations of aircraft rotation speed are demonstrated using safety windows and safety distribution pie charts.

4 Conclusion

A generalized methodology has been developed for mapping an aircraft's flight safety performance in multi-factor situations. Safety windows and other types of safety 'topology' knowledge maps have been implemented and demonstrated using VATES M&S tool.

These intelligent formats can serve as a medium for a 'bird's eye view' level mapping, depiction and prediction of flight safety under uncertainty. In this process, both physics and logic of a multi-factor 'what-if' neighborhood built around a given baseline situation is explored. The goal is to enhance the situational knowledge base and the decision-making mechanism of an operator (a pilot or automaton) in emergencies.

Safety windows are expedient to integrate with other advanced techniques and technologies, such as MDO systems, FMEA tools, vehicle health-monitoring systems, multimodal sensors, and virtual-reality based pilot-vehicle interface. The goal is to help design reliable and affordable flight control and flight safety protection systems. These systems must be capable to recognize and remedy both known and unknown yet multifactor accident patterns. This list includes (but not limited to) the following situation types: LOC, CFIT, 'pilot error', '9/11', midair collision, and other scenarios.

The developed methodology can be applied to the following problem fields: advanced examination of the combined effect of aerodynamics, flight control and operational factors on the aircraft flight dynamics in design; knowledge-centered training of line pilots, test pilots and pilot instructors; design of terrorist-/ fool-proof flight safety protection systems; research into autonomous collision avoidance of aircraft in close 'free flight' airspace, intelligent flight control for manned and unmanned aerospace vehicles under uncertainty.

Acknowledgements

References

[1] Burdun I.Y. UAV 'Built-in' Safety Protection: A Knowledge-Centered Approach. *Proc. of AUVSI Unmanned Systems Europe 2007 Conference & Exhibition, 8-9 May 2007,* Köln, Germany, 49 pp, 2007.

[2] Бурдун Е.И. Прогнозирование безопасности полёта самолета гражданской авиации в сложных условиях. *Автореферат диссертации на соискание ученой степени доктора инженерных наук*, РТУ, Рига, 36 с, 2008 [in Russian].

[3] Burdun I.Y. A Technique for Aircraft «Built-In» Safety Protection in Complex (Multifactor) Conditions Based on Situational Modeling and Simulation. *Proc. Of VIII International Conference 'System Identification and Control Problems', V.A. Trapeznikov Institute of Control Sciences, Russian Academy of Sciences, January 26-30, 2009,* Moscow, Russia, 44 pp, 2009. [in Russian].

[4] Burdun I.Y. The Intelligent Situational Awareness And Forecasting Environment (The S.A.F.E. Concept): A Case Study. *Proc. of 1998 SAE Advances in Flight Safety Conference and Exhibition, April 6-8, 1998*, Daytona Beach, FL, USA, Paper 981223, pp 131-144, 1998.

[5] Программно-моделирующий комплекс (ПМК) для исследований безопасности поведения системы «оператор (лётчик, автомат) – летательный аппарат (ЛА) – эксплуатационная среда» в сложных (многофакторных) полётных ситуациях (ПМК VATES). *Свидетельство об официальной регистрации программы для ЭВМ № 2007613256, выданное Федеральной службой по интеллектуальной собственности, патентам и товарным знакам РФ. Правообладатель: ООО «ИНТЕЛОНИКА». Автор: Бурдун И.Е. Зарегистрировано в Реестре программ для ЭВМ 02.08.2007*, Москва, 1 с, 2007 [VATES Patent, in Russian].

Contact Author Email Address

info@intelonics.com, or ivan.burdun@mail.ru.

Copyright Statement

S_0: Normal takeoff

S_1: Takeoff, wet runway

S_2: Continued takeoff, wet runway

S_3: Continued takeoff, wet runway, and wind shear

S_4: Continued takeoff, wet runway, wind shear, and pilot error

S_5: 'Chain reaction' type situation

Φ_9 Wet (slippery) runway

Φ_4 Engine failure at V_1

Φ_7 Wind shear after lift-off

Φ_6 Pilot error (e.g. bank control)

Φ_8 Automatic control logic error

anomalous but very dangerous combination of operational factors resulting in a 'chain reaction' accident

catastrophic state

safe state

Legend:

Φ_4, Φ_6, Φ_7, Φ_8, Φ_9 – operational/design factors (or risk/ 'what-if'/ flight path branching factors)

– colors for coding flight situation safety levels

– 'bud'-type event for 'implanting' additional operational factors into flight situation scenario

S_0, S_1, …, S_5 – notional examples of flight situation scenarios in the order of increasing complexity and operational risk

$\Omega(\Phi|S_k)$ – subset of operational factors affecting scenario S_k, $k = 0, 1, …, 5$: $\Omega(S_0) = \varnothing$, $\Omega(\Phi|S_1) = \{\Phi_9\}$, $\Omega(\Phi|S_2) = \{\Phi_4, \Phi_9\}$, $\Omega(\Phi|S_3) = \{\Phi_4, \Phi_7, \Phi_9\}$, $\Omega(\Phi|S_4) = \{\Phi_4, \Phi_6, \Phi_7, \Phi_9\}$, $\Omega(\Phi|S_5) = \{\Phi_4, \Phi_6, \Phi_7, \Phi_8, \Phi_9\}$

Fig. 1. Multifactor Flight Situation Build-up Model (Takeoff Example)

Basic elements

'Micro-structure' of flight (situation scenario graph)

'Macro-structure' of flight (situational tree)

Event Process

E   **Π**

Elementary situation

Legend:

E_i – event

Π_j – process

C – fuzzy constraint

○ – reference/ check state ('node')

● – branch grafting state ('bud')

◇ – branch's target state ('leaf')

△ – branch's source state ('root')

B_{-1} – parent branch

B_0 – main branch ('trunk') – baseline flight situation scenario

B_n – n-th order derivative branch, complex flight situation scenario with n contributing operational factors, $n = 1, 2, …$

Fig. 2. Two-Level Memory-Based Model of Complex (Multifactor) Flight Situations Domain

student pilot   interim (immature) states of experience   professional pilot, ace pilot, test pilot

1   2   3   4   5   6   7   8   9   10

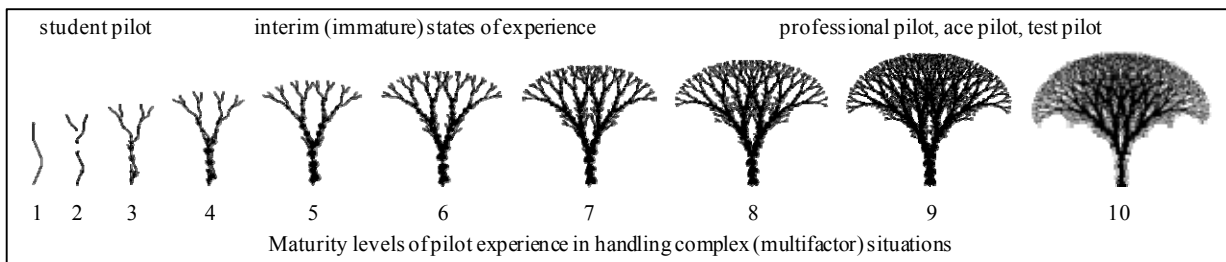Maturity levels of pilot experience in handling complex (multifactor) situations

Fig. 3. Fractal Tree Growth Dynamics as Illustration of Human Pilot's Situational (Tactical) Experience Development in Long-Term Memory

Legend:
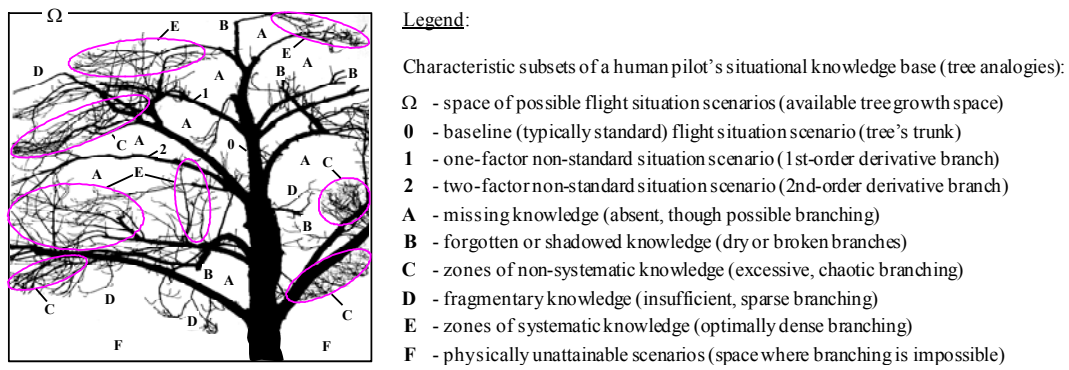
Characteristic subsets of a human pilot's situational knowledge base (tree analogies):

Ω - space of possible flight situation scenarios (available tree growth space)

0 - baseline (typically standard) flight situation scenario (tree's trunk)

1 - one-factor non-standard situation scenario (1st-order derivative branch)

2 - two-factor non-standard situation scenario (2nd-order derivative branch)

A - missing knowledge (absent, though possible branching)

B - forgotten or shadowed knowledge (dry or broken branches)

C - zones of non-systematic knowledge (excessive, chaotic branching)

D - fragmentary knowledge (insufficient, sparse branching)

E - zones of systematic knowledge (optimally dense branching)

F - physically unattainable scenarios (space where branching is impossible)

Fig. 4. Natural Tree Based Analogy of Main Defects of Human Pilot's Situational 'Knowledge Base'

Fig. 5. Joint Graph of Baseline (Tree Trunk) Flight Situation Scenarios
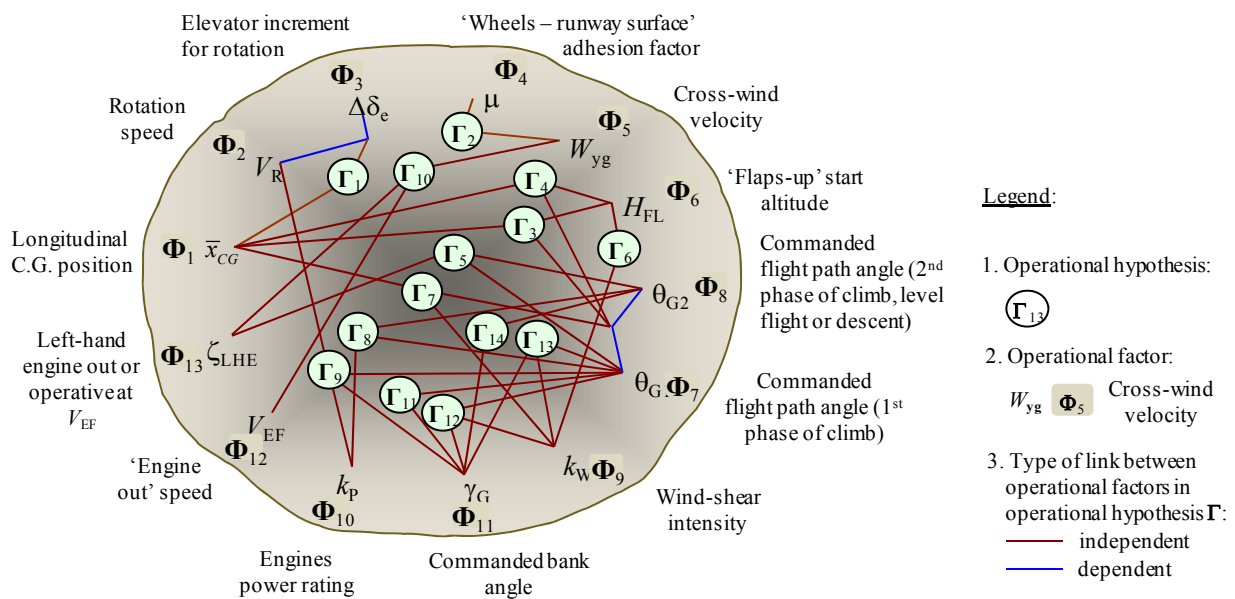
Fig. 6. Operational Factors Selected for Testing. Design Field of Operational Hypotheses
(Ground-roll, Takeoff, Initial Climb, Level Flight, Descent)

(a) Safety Palette

- turquoise ('optimum'), ξ_G
- green ('norm'), ξ_G
- yellow ('attention'), ξ_Y
- red ('danger'), ξ_R
- black ('fatal'), ξ_B
- gray/white ('unknown'), ξ_W
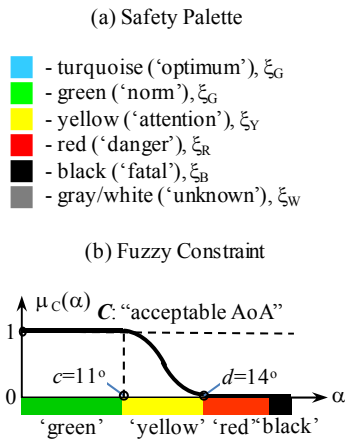
(b) Fuzzy Constraint

Legend: c, d – characteristic points of fuzzy constraint C carrier; $\mu_C(x)$ – L.A. Zadeh fuzzy set membership function
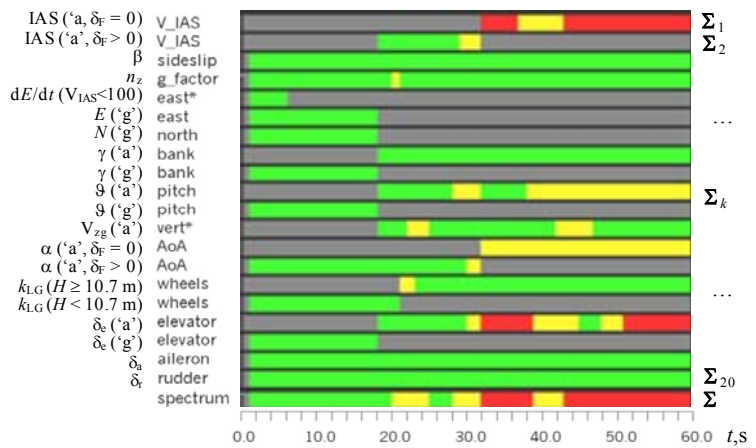
Legend: See Fig. 7. Σ_k – partial safety spectrum constructed for variable x_k, $k = 1$, …, p; $p = 20$; Σ – integral safety spectrum; 'a' – airborne, 'g' – ground-roll, { β, E, N, γ, ϑ, V_{zg}, α, k_{LG}, δ_e, δ_a, δ_r, H } – system model variables.

Fig. 7. Safety Palette (a) and Fuzzy Constraint (b) Concepts

Fig. 8. Examples of Safety Spectra for 'Flight' F_{2782}: "Normal Takeoff, Initial Climb at $\theta_G=16^o$ and $\gamma_G=22.5^o$, 'Very Strong' Wind-Shear"
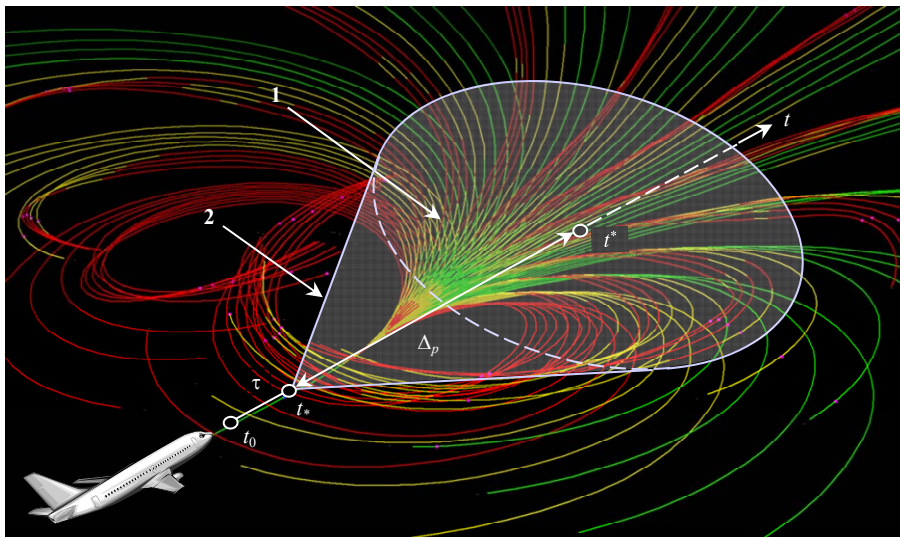
Legend:

1 – situational tree used for short-term prediction of flight safety
2 – multifactor domain safety analysis cone (forecast sub-tree)
t_o – current flight time
t_* – forecast start time
t^* – forecast stop time
$\tau = (t_* - t_o)$ – decision making delay
$\Delta_p = (t^* - t_*)$ – prediction depth
■■■■ – integral safety spectra colors

Fig. 9. Situational Tree $S_1 \cdot \Gamma_{11}$: "Takeoff and Initial Climb, 'Strong' Wind-Shear, Flight Path and Bank Angles Control Errors"
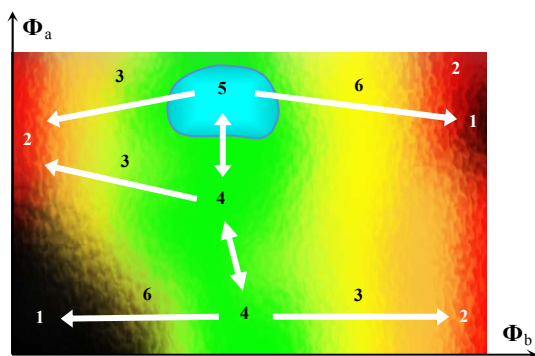
Legend:

Φ_a, Φ_b – key operational factors (safety window's coordinates)
1 – 'abyss' (catastrophe)
2 – 'hill' (danger)
3 – 'slope' (reversible state transitions)
4 – 'valley' (standard safety, norm)
5 – 'lake' (maximum safety/mission effectiveness, optimum)
6 – 'precipice' (abrupt, irreversible state transitions, 'chain reaction')
I II-a II-b III IV V – safety classification categories

Fig. 10. Main Objects of Flight Safety 'Topology'

(a) Flight Safety Windows
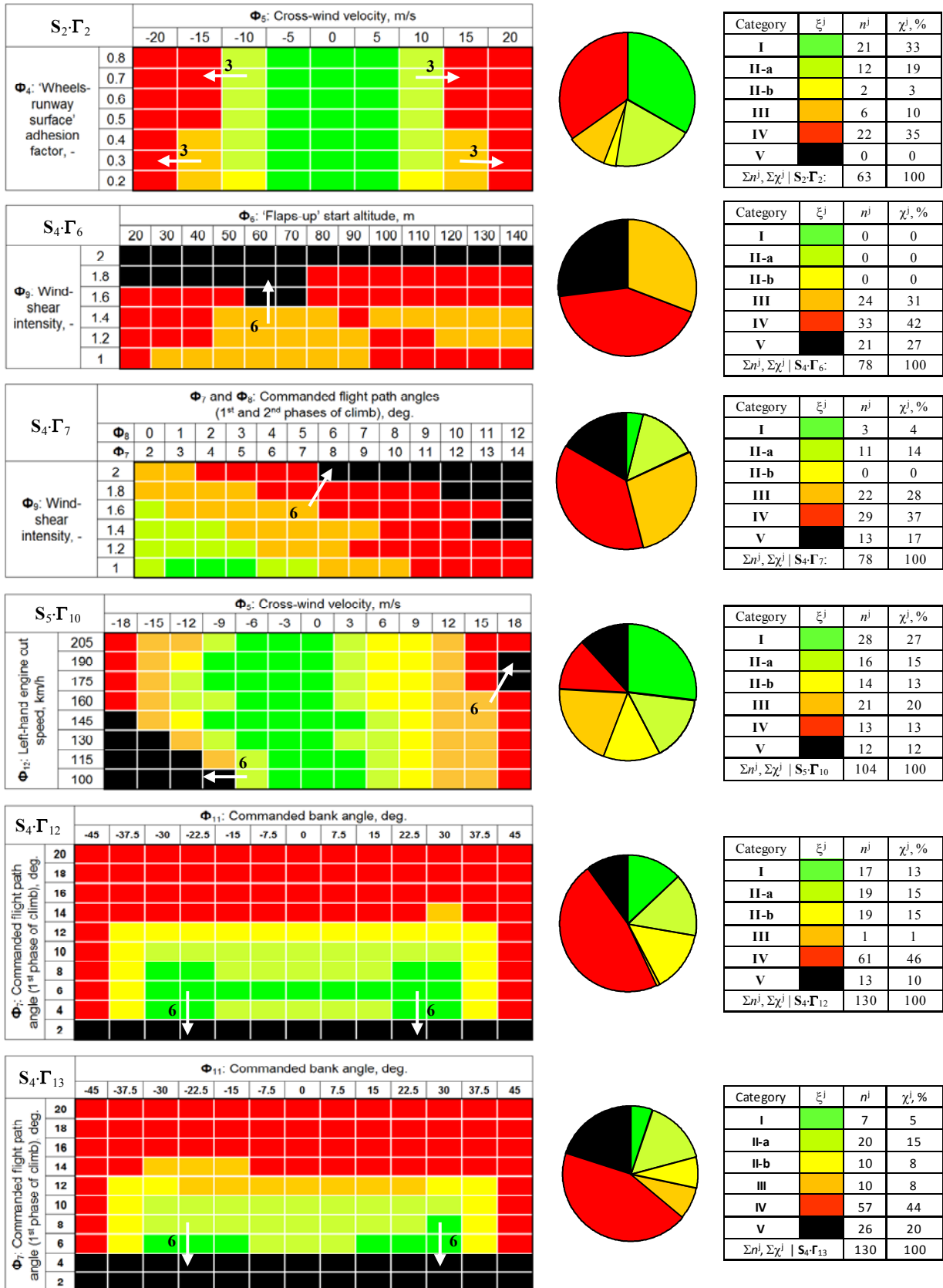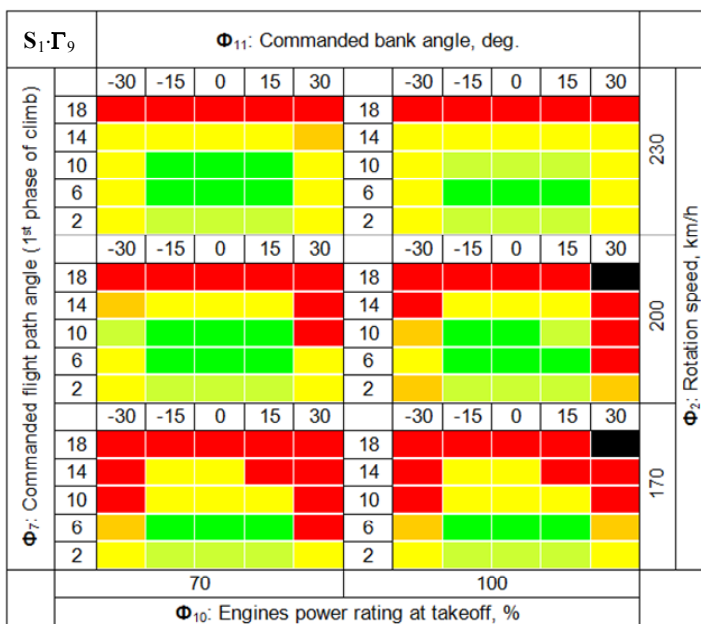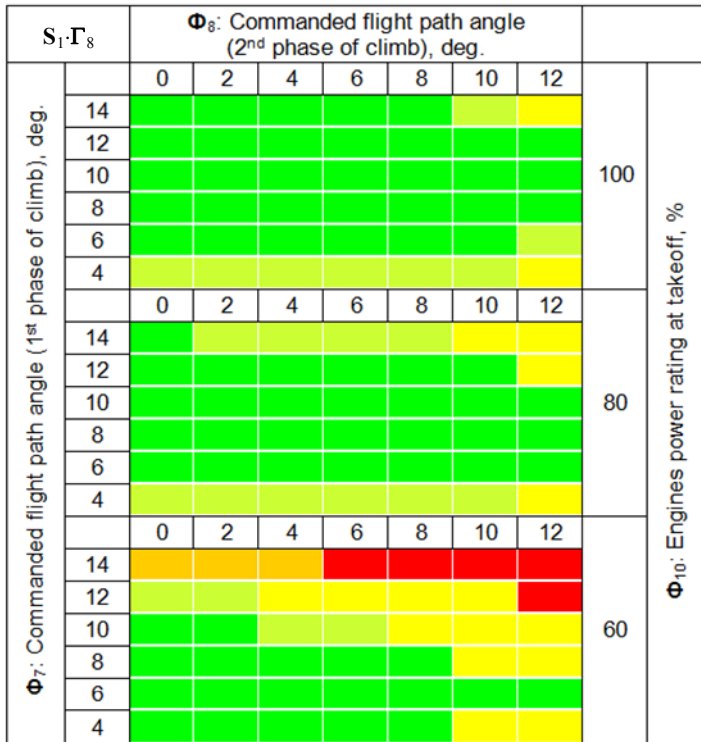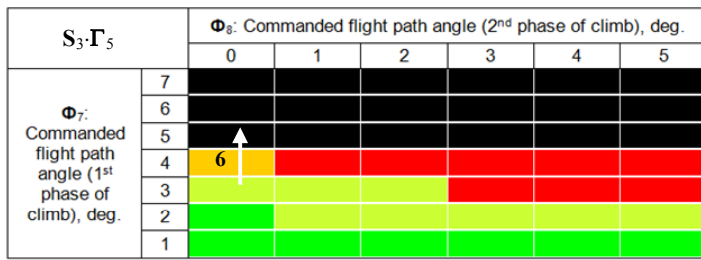
(b) Safety Chances Distribution Charts

Fig. 11. Flight Safety Windows (a) and Safety Chances Distribution Charts (b) for Selected Compositions $\mathbf{S}_i \cdot \boldsymbol{\Gamma}_k$

(a) Flight Safety Windows
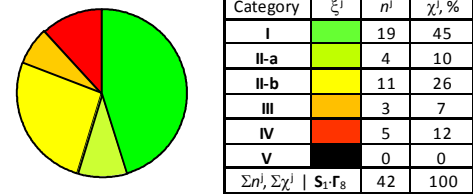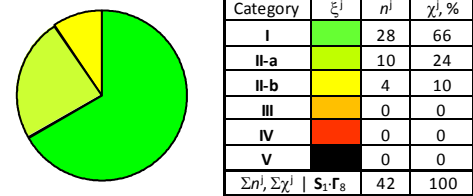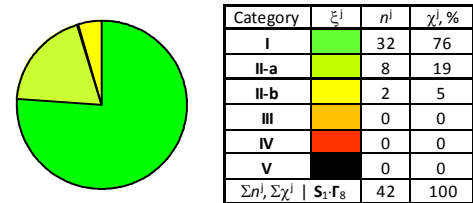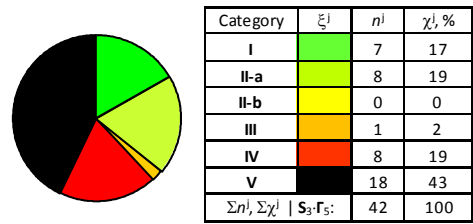
(b) Safety Chances Distribution Charts
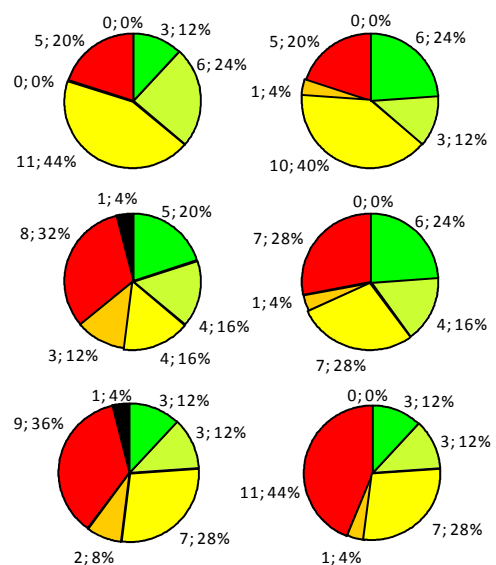
Fig. 11 (continued). Flight Safety Windows (a) and Safety Chances Distribution Charts (b) for Selected Compositions $\mathbf{S}_i \cdot \boldsymbol{\Gamma}_k$